Constrained nanoparticles deliver siRNA and sgRNA to T cells *in vivo* without targeting ligands

Melissa P. Lokugamage[1*], Cory D. Sago[1,2*], Zubao Gan[1], Brandon Krupzak[1,2], James E. Dahlman[1,2]

[1]Wallace H. Coulter Department of Biomedical Engineering, Georgia Institute of Technology, Atlanta, GA, 30332, USA

[2]Current Address: Guide Therapeutics, Atlanta, GA, 30332, USA

*These authors contributed equally

Correspondence: james.dahlman@bme.gatech.edu

Abstract

T cells help regulate immunity, which makes them an important target for RNA therapies. While nanoparticles carrying RNA have been directed to T cells *in vivo* using protein- and aptamer-based targeting ligands, systemic delivery to T cells without targeting ligands remains challenging. Given that T cells endocytose lipoprotein particles and enveloped viruses, two natural systems with structures that can be similar to lipid nanoparticles (LNPs), we hypothesized LNPs devoid of targeting ligands could deliver RNA to T cells *in vivo*. To test this hypothesis, we quantified how 168 nanoparticles delivered siRNA to 9 cell types *in vivo* using a novel siGFP-based barcoding system and bioinformatics. We found nanomaterials containing conformationally constrained lipids formed stable LNPs, herein named constrained lipid nanoparticles (cLNPs). cLNPs delivered siRNA and sgRNA to T cells at doses as low as 0.5 mg / kg, and unlike previously reported LNPs, did not preferentially target hepatocytes. Delivery occurred via a chemical composition-dependent, size-independent mechanism. These data suggest the degree to which lipids are constrained alters nanoparticle targeting. They also suggest natural lipid trafficking pathways can promote T cell delivery, offering an alternative to active targeting approaches.

Materials and Methods

Nanoparticle Formulation. Nanoparticles were formulated using a microfluidic device[1] as previously described. Briefly, nucleic acids (siRNA, sgRNA and DNA barcodes) were diluted in citrate buffer while lipid-amine compounds, alkyl tailed PEG, cholesterol, and DSPC were diluted in 100% ethanol. PEG, cholesterol, and DSPC was purchased from Avanti Lipids. Citrate and ethanol phases were combined in a microfluidic device by syringe pumps at a relative flow rate of 3:1.

DNA Barcoding. Each chemically distinct LNP was formulated to carry its own unique DNA barcode and siRNA. For example, LNP1 carried DNA barcode 1 and siGFP, while the chemically distinct LNP2 carried DNA barcode 2 and siGFP. Single stranded DNA sequences were purchased from Integrated DNA Technologies. To ensure equal amplification of each sequence, we included universal forward and reverse primer regions. Each barcode was distinguished using a unique 8 nucleotide sequence. We used 156 distinct sequences designed to prevent sequence 'bleaching' on the Illumina MiniSeq sequencing machine.

Nanoparticle Characterization. LNP hydrodynamic diameter was measured using a plate reader formatted dynamic light scattering machine (Wyatt). LNPs were diluted in sterile 1X PBS to a

concentration of ~0.06 μg/mL and analyzed. LNPs were only included if they formed monodisperse populations with diameter between 20 and 200nm. Particles that met these criteria were dialyzed with 1X phosphate buffered saline (PBS, Invitrogen), and were sterile filtered with a 0.22 μm filter.

Animal Experiments. All animal experiments were performed in accordance with the Georgia Institute of Technology's IACUC. C57BL/6J (#000664), GFP (#003291), and constitutive SpCas9 (#026179) mice were purchased from The Jackson Laboratory and used between 5-12 weeks of age. In all experiments, we used N=3-5 mice/group. Mice were injected intravenously via the lateral tail vein. The nanoparticle concentration was determined using NanoDrop (Thermo Scientific).

Cell Isolation & Staining. Cells were isolated 72 hours (for screens and siRNA silencing) or 120 hours (for *in vivo* Cas9 gene editing) hours after LNP injection unless otherwise noted. Mice were perfused with 20 mL of 1X PBS through the right atrium. As we previously described[2, 3], tissues were cut and placed in a digestive enzyme solution with Collagenase Type I (Sigma Aldrich), Collagenase XI (Sigma Aldrich) and Hyaluronidase (Sigma Aldrich) at 37 ºC for 45 minutes. Cell suspension was filtered through 70μm mesh and red blood cells were lysed. Cells were stained to identify populations and sorted using the BD FacsFusion in the Georgia Institute of Technology Cellular Analysis Core for *in vivo* experiments. The antibody clones used were: anti-CD31 (390, BioLegend), anti-CD45.2 (104, BioLegend), anti-CD68 (FA-11, BioLegend), anti-CD19 (6D5, Biolegend), anti-CD3 (17A2, Biolegend), anti-CD8a (53-6.7, Biolegend), and anti-CD4 (GK1.5, Biolegend). Representative FACS plots are found in Supporting Information Figure 3.

PCR Amplification for Illumina Sequencing. All samples were amplified and prepared for sequencing using nested PCR. 2 μL of primers were added to 5 μL of Kapa HiFi 2X master mix, and 3 μL template DNA/water. The second PCR added Nextera XT chemistry, indices, and i5/i7 adapter regions. Dual-indexed samples were run on a 2% agarose gel to ensure that PCR reaction occurred before being pooled and gel purified.

Deep Sequencing. Illumina sequencing was conducted in Georgia Institute of Technology's Molecular Evolution core. Runs were performed on an Illumina Miniseq. Primers were designed based on Nextera XT adapter sequences.

Barcode Sequencing Normalization. Counts for each particle, per cell type, were normalized to the barcoded LNP mixture applied to cells or injected into the mouse.

TNS Assay. The pKa of 11-A-M and 1-A-N was measured as previously described[3]. Briefly, a stock solution of 10mM HEPES (Sigma), 10mM MES (Sigma), 10mM sodium acetate (Sigma), and 140nM sodium chloride (Sigma) was prepared and pH adjusted with hydrogen chloride and sodium hydroxide to a range of pH between 4 and 10. Using 4 replicates for each nanoparticle at each pH, 140 µL pH-adjusted buffer was added to a 96-well plate, followed by the addition 5 µL of 2-(p-toluidino)-6-napthalene sulfonic acid (60 µg / mL). 5uL of each nanoparticle was added to each well. After 5 minutes of incubation under gentle shaking, fluorescence absorbance was measured using excitation wavelengths of 325 nm and emission wavelength of 435nm.

RNA interference. siRNAs were chemically modified at the 2' position to increase stability and negate immunostimulation. Seventy-two hours after injection, tissues were isolated and protein expression was determined via flow cytometry. GFP mean fluorescent intensity in PBS-treated mice was made 100%, and GFP expression in treated mice was normalized to that value.

***In vivo* Cas9 Editing.** Mice constitutively expressing SpCas9 were injected with cLNP carrying 2 mg / kg of sgGFP. 5 days after injection, cells were isolated via FACS.

Data Analysis & Statistics. Sequencing results were processed using a custom R script to extract raw barcode counts for each tissue. These raw counts were then normalized with an R script prior for further analysis. Statistical analysis was done using GraphPad Prism 7; more specifically Paired 2-tail T-test or One-way ANOVAs were used where appropriate. Data is plotted as mean ± standard error mean unless otherwise stated.

Data Access. All data are available upon request to james.dahlman@bme.gatech.edu.

Acknowledgements

The authors thank the Anton Bryksin and the employees at the Georgia Tech Molecular Evolution Core. J.E.D. also thanks Taylor E. Shaw.

Funding

Funding was provided by the Georgia Tech startup (awarded to J.E.D.); Sangamo Therapeutics Sponsored Research (awarded to J.E.D.); Coulter Translational Award (awarded to J.E.D.); Parkinson's Disease Foundation PDF-JFA-1860 (awarded to J.E.D.); the NIH / NIGMS-sponsored Computational Biology and Predictive Health Genomics Training Program T32GM105490 (awarded to M.P.L.); the NIH / NIGMS-sponsored Immunoengineering Training Grant T32EB021962 (awarded to C.D.S.)

Author Contributions

M.P.L., C.D.S., Z.G., and J.E.D. conceived the experiments. M.P.L., C.D.S., Z.G., B.K., and J.E.D. performed experiments. M.P.L., C.D.S., and J.E.D. wrote the paper. Z.G., and B.K., edited and approved the paper.

Competing Financial Interests

M.P.L., C.D.S., Z.G., and J.E.D. have filed intellectual property related to this publication. C.D.S. and J.E.D. are co-founders of Guide Therapeutics.

Detailed Methods Citations

[1] D. Chen, K. T. Love, Y. Chen, A. A. Eltoukhy, C. Kastrup, G. Sahay, A. Jeon, Y. Dong, K. A. Whitehead, D. G. Anderson, J Am Chem Soc 2012, 134, 6948.
[2] K. Paunovska, C. D. Sago, C. M. Monaco, W. H. Hudson, M. G. Castro, T. G. Rudoltz, S. Kalathoor, D. A. Vanover, P. J. Santangelo, R. Ahmed, A. V. Bryksin, J. E. Dahlman, Nano Lett 2018, 18, 2148.
[3] J. E. Dahlman, C. Barnes, O. F. Khan, A. Thiriot, S. Jhunjunwala, T. E. Shaw, Y. Xing, H. B. Sager, G. Sahay, L. Speciner, A. Bader, R. L. Bogorad, H. Yin, T. Racie, Y. Dong, S. Jiang, D. Seedorf, A. Dave, K. Singh Sandhu, M. J. Webber, T. Novobrantseva, V. M. Ruda, K. R. Lytton-JeanAbigail, C. G. Levins, B. Kalish, D. K. Mudge, M. Perez, L. Abezgauz, P. Dutta, L. Smith, K. Charisse, M. W. Kieran, K. Fitzgerald, M. Nahrendorf, D. Danino, R. M. Tuder, U. H. von Andrian, A. Akinc, D. Panigrahy, A. Schroeder, V. Koteliansky, R. Langer, D. G. Anderson, Nat Nano 2014, 9, 648.

Supplementary Figure 1. A) General synthesis for lipid 11A. B) Mass and NMR data for key ionizable lipids. C) ^{1}H NMR spectra for Lipid 11A. D) ^{13}C NMR spectra for Lipid 11A.

A

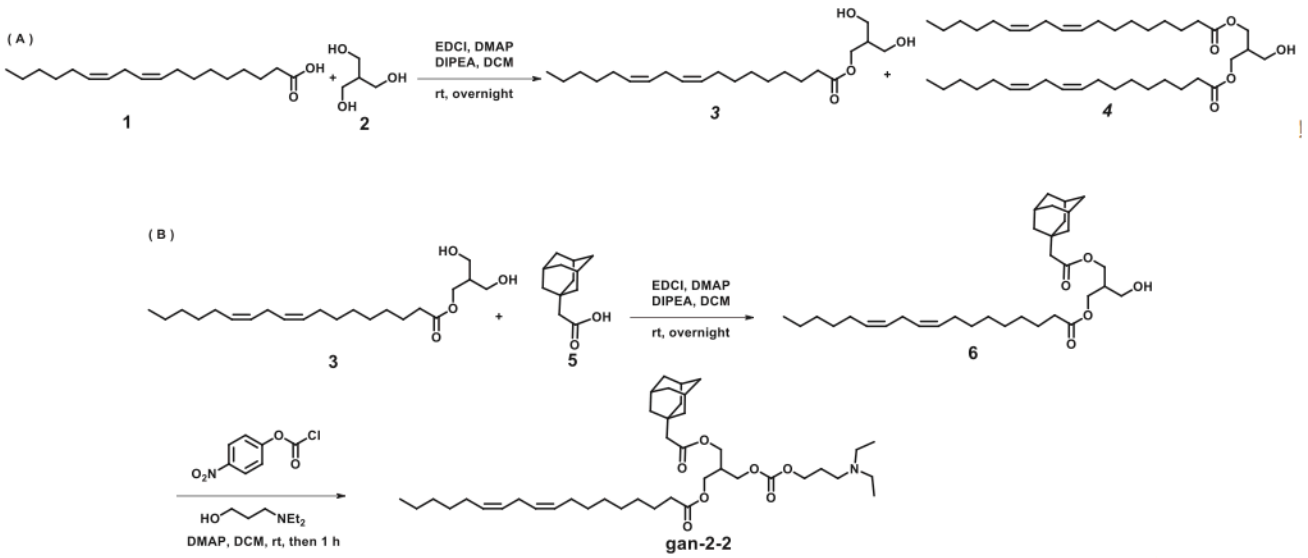

11A: To a solution of linoleic acid 1 (4.0 g, 14.2 mmol), 4-dimethylaminopyridine (DMAP) (0.4 g, 2.9 mmol), N, N-diisopropylethylamine (DIPEA) (3.7 mL, 20.5 mmol) and 2-(hydroxymethyl) propane-1,3-diol (1.5 g, 14.2 mmol) in anhyd. CH2Cl2 (40 mL) under nitrogen atmosphere was added N-(3-dimethylaminopropyl)-N'-ethylcarbodiimide hydrochloride (EDCI) (4.1 g, 20.5 mmol) at 25 °C. The reaction mixture was stirred at room temperature for overnight and linoleic acid 1 was consumed completely monitored by TLC, then the reaction mixture was directly concentrated under reduced pressure. Purification of the crude residue via silica gel flash column chromatography (gradient eluent: 1-30% of EtOAc/hexane) afforded compound 3 (2.3 g, 44% yield) and compound 4 (1.7 g, 30% yield) as colourless oil.

To a solution of compound 3 (150 mg, 0.41 mmol), DMAP (10 mg, 0. 1 mmol), DIPEA (0.1 mL, 0.6 mmol) and adamantane (79 mg, 0.41 mmol) in anhyd. CH2Cl2 (2 mL) under nitrogen atmosphere was added EDCI (114 mg, 0.6 mmol). The reaction mixture was stirred at room temperature for overnight. and compound 3 was consumed completely monitored by TLC, then the reaction mixture was directly concentrated under r educed pressure. Purification of the crude residue via silica gel flash column chromatography (gradient eluent: 0-20% of EtOAc/hexane) afforded compound 6 (103 mg, 53% yield) as colourless oil.

To a solution of compound 6 (76 mg, 0. 16 mmol) and DMAP (45 mg, 0. 37 mmol) in anhyd. CH2Cl2 (2 mL) under nitrogen atmosphere was added 4-nitrophenylchloroformate (65 mg, 0. 32 mmol). After stirring at room temperature for 1 hour, 3-diethylamino-1-propanol (0.44 mL, 0.96 mmol) was added into the reaction mixture and then stirred at room temperature for 1 hour. The reaction mixture was directly concentrated under reduced pressure. Purification of the crude residue via silica gel flash column chromatography (gradient eluent: 0-4% of MeOH /DCM) afforded compound 11A (32 mg, 29% yield) as colorless oil.

B

Lipid-1C: HRMS (ESI, m/z) calculated for $C_{48}H_{84}NO_7$ $[M + H]^+$: 786.6242, found 786.6227.

Lipid-2C: HRMS (ESI, m/z) calculated for $C_{49}H_{87}N_2O_7$ $[M + H]^+$: 815.6508, found 815.6494.

Lipid-3C: HRMS (ESI, m/z) calculated for $C_{46}H_{73}N_2O_6S$ $[M + H]^+$: 781.5187, found 781.5187.

Lipid-4C: HRMS (ESI, m/z) calculated for $C_{48}H_{84}NO_8$ $[M + H]^+$: 802.6191, found 802.6194.

Lipid-5C: HRMS (ESI, m/z) calculated for $C_{48}H_{75}N_2O_6$ $[M + H]^+$: 775.5620, found 775.5645.

Lipid-6C: HRMS (ESI, m/z) calculated for $C_{45}H_{74}N_3O_6$ $[M + H]^+$: 752.5572, found 752.5586.

Lipid-7C: HRMS (ESI, m/z) calculated for $C_{45}H_{73}N_2O_6$ $[M + H]^+$: 737.5463, found 737.5476.

Lipid-8C: HRMS (ESI, m/z) calculated for $C_{49}H_{75}N_2O_6$ $[M + H]^+$: 787.5620, found 787.5628.

Lipid-9C: HRMS (ESI, m/z) calculated for $C_{43}H_{76}NO_6$ $[M + H]^+$: 702.5667, found 702.5686.

Lipid-10C: HRMS (ESI, m/z) calculated for $C_{47}H_{76}BO_8$ $[M + H]^+$: 779.5628, found 779.5628.

Lipid-11C: HRMS (ESI, m/z) calculated for $C_{48}H_{86}NO_7$ $[M + H]^+$: 788.6399, found 788.6412.

Lipid-11B: HRMS (ESI, m/z) calculated for $C_{50}H_{94}NO_9$ $[M + H]^+$: 852.6923, found 852.6903.

Lipid-11A. HRMS (ESI, m/z) calculated for $C_{42}H_{72}NO_7$ $[M + H]^+$: 702.5303, found 702.5277.

^{1}H NMR (500 MHz, $CDCl_3$) δ 0.89 (t, J = 7.0 Hz, 3 H), 1.24-1.36 (m, 22 H), 1.57-1.62 (m, 10 H), 1.64 (s, 2 H), 1.69 (s, 2 H), 1.72 (s, 1 H), 1.97 (s, 2 H), 2.01-2.09 (m, 8 H), 2.31 (t, J = 7.5 Hz, 2 H), 2.43 (m, 1 H), 2.77 (t, J = 6.5, 2 H), 2.89 (m, 4 H), 4.15 (dd, J_1 = 6.0 Hz, J_2 = 13.5 Hz, 4 H), 4.21 (m, 4 H), 5.36 (m, 4 H); ^{13}C NMR (125 MHz, $CDCl_3$) δ 14.0, 14.2, 22.5, 24.8, 25.6, 27.2, 29.1, 29.3,29.6, 29.7, 31.5, 31.9, 32.8, 34.1, 36.6, 37.4, 42.4, 46.7, 48.7, 49.1, 61.0, 61.1, 61.3, 61.4, 64.2, 65.1, 65.3, 65.8, 127.9, 128.0, 130.0, 130.2, 154.7, 171.4, 173.5;

!

C

11A

^{1}H-NMR (500MHz, $CDCl_3$)

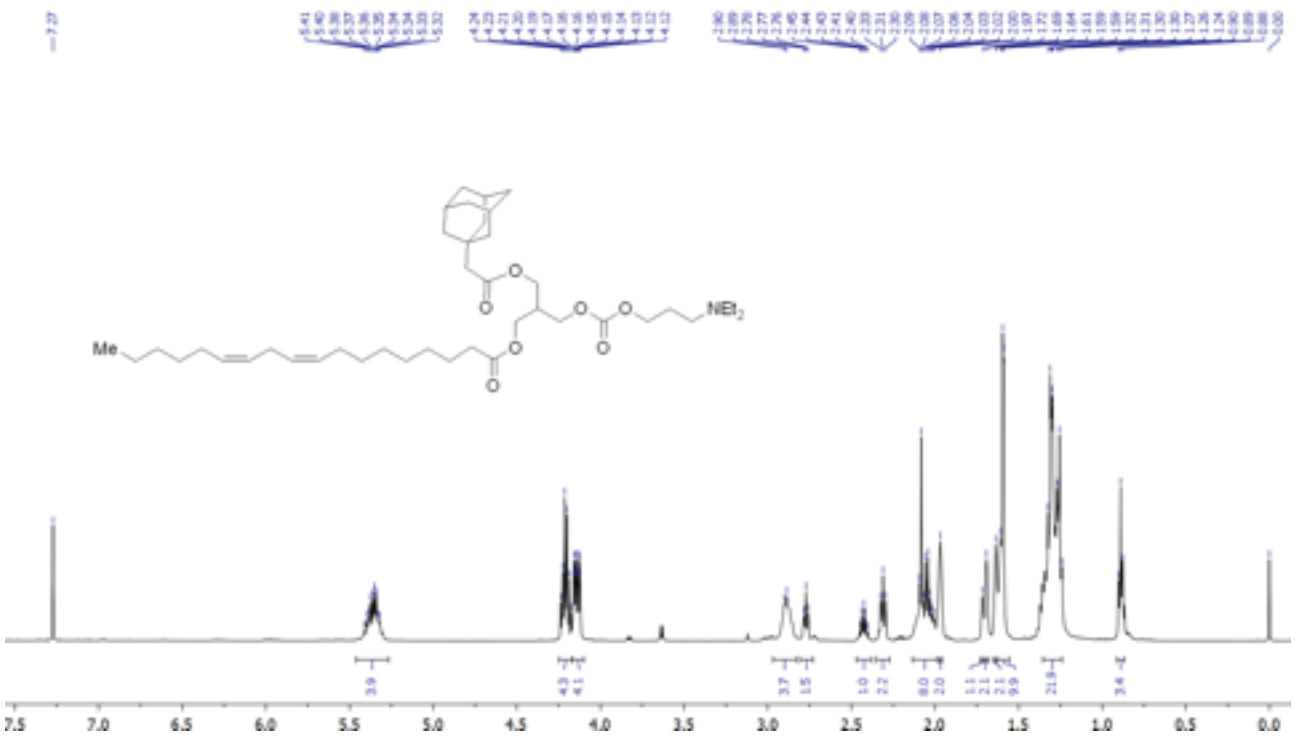

D

11A

^{13}C-NMR (125MHz, $CDCl_3$)

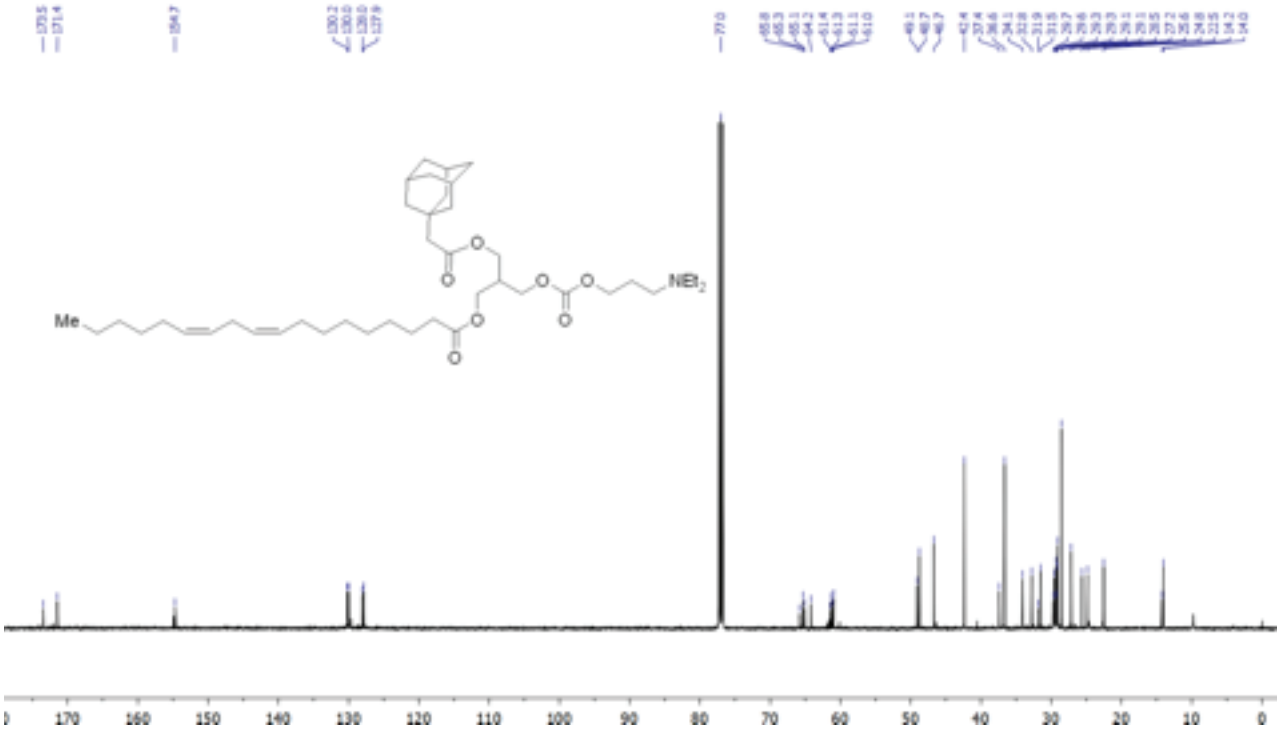

Supplementary Figure 2. A) Sequence and chemical modifications of siGFP. Hydrodynamic diameter of LNPs plotted as a function of B) ionizable lipid type, C) molar percent of ionizable lipid, and D) phospholipid type.

A

siGFP sense: 5′ - AcAuGAAGcAGcACGACuU dT sdT - 3′
siGFP antisense: 5′ - AAGUCGUGCUGCUUCAUGU dT sdT -3′

A, G, U, C: RNA nucleotide
dT: deoxy-T
a, g, u, c: 2′-O-Methyl nucleotide
s: phosphorothioate

B

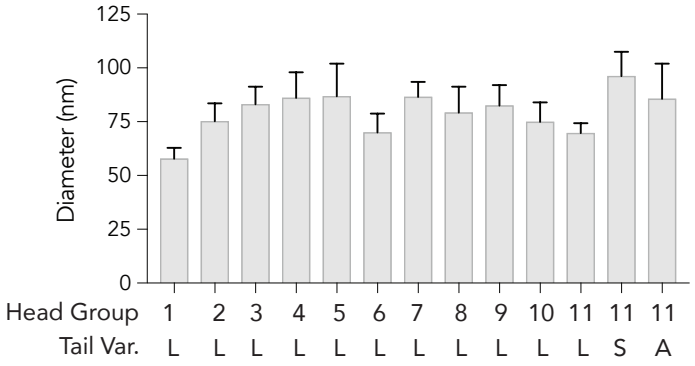

C

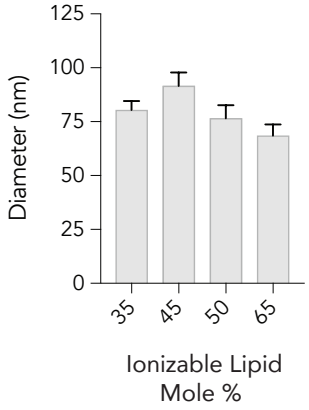

D

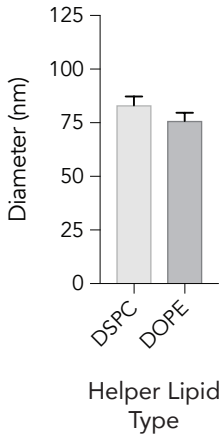

Supplementary Figure 3. A) Representative FACs plots showing gating strategy for splenic CD3+ T cells. B) Cell-type specific markers.

A

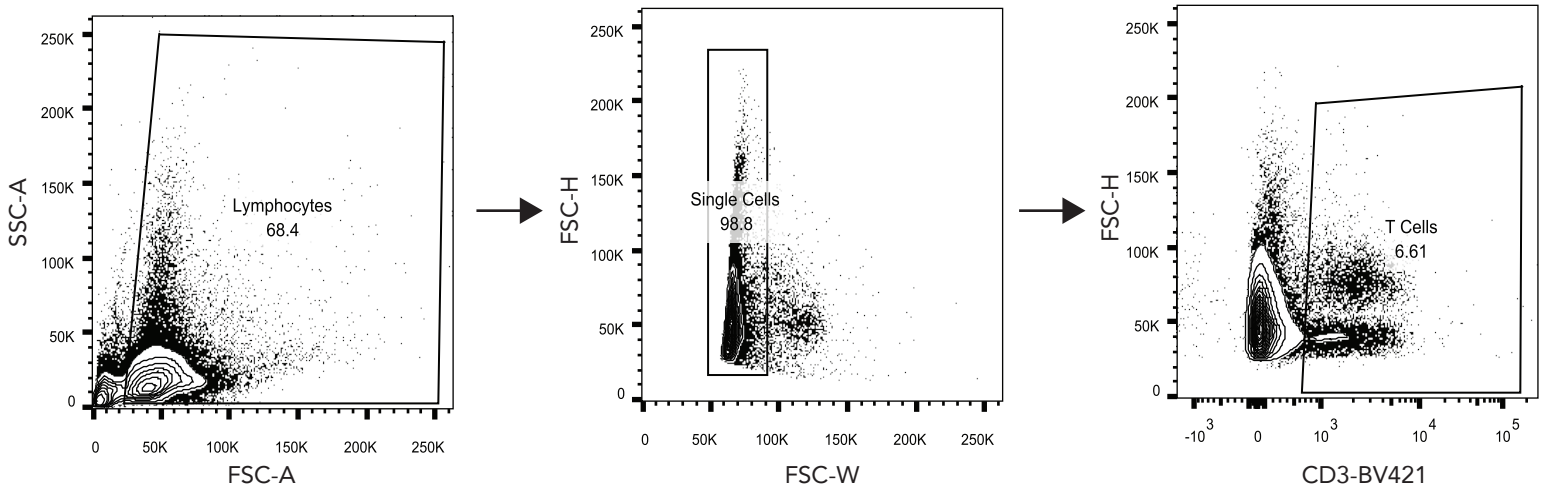

B

Cell Type	FACS Markers	Tissue
Endothelial cells	CD31+ CD45-	*L , M , v*
Immune Cells	CD31- CD45+ CD11b-	*L , M , v*
T Cells	CD3+ CD19-	*S*
B Cells	CD3- CD19+	*S*
Hepatocytes	CD31- CD45- CD68-	*v*
Kupffer Cells	CD31- CD45+ CD68+	*v*

Lung, ***M***arrow, ***S***pleen, Li***v***er

Supplementary Figure 4. A) An example showing how enrichment is calculated.

A

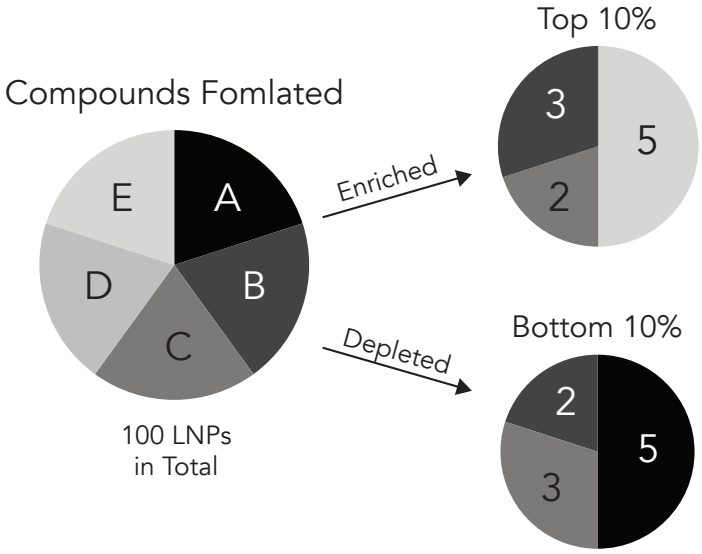

$$\frac{\text{\# of Compound N in Top or Bottom 10\%}}{\text{Total \# LNPs} \times 10\%} \div \frac{\text{\# of Compound N Formulated}}{\text{Total \# LNPs}} = \text{Enriched or Depleted}$$

Total Enrichment = Enriched - Depleted

Supplementary Figure 5. A) Normalized DNA delivery of LNPs plotted as a function of phospholipid. 2-way T test, **P<0.01. (B) Paired analysis of normalized DNA delivery of LNPs containing DSPC or DOPE. Paired 2-way T test, *P<0.05.

A

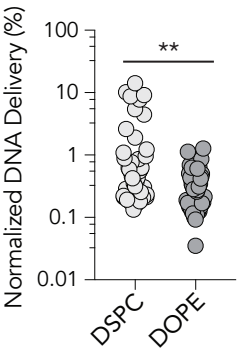
Normalized DNA Delivery (%)
100
10
1
0.1
0.01
**
DSPC
DOPE

B

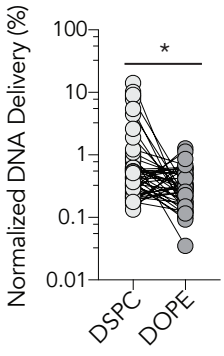
Normalized DNA Delivery (%)
100
10
1
0.1
0.01
*
DSPC
DOPE

Supplementary Figure 6. A) Physical and chemical analysis of headgroups. B) Correlation of headgroup molecular weight and enrichment. C) Correlation of headgroup LogP and enrichment. D) Correlation of headgroup polar surface area and enrichment. E) Normalized delivery of LNPs formulated with different ionizable lipids sharing headgroup 11, but with different tail structures. F) Correlation of LNP diameter and normalized DNA delivery.

A

Lipomer	Molecular Weight of Head Group	LogP of Head Group	Total Polar Surface Area of Head Group	Enrichment in T Cells
Gan-1-105	158	0.62	29.5	-1.3
Gan-1-106	156	0.26	29.5	3.9
Gan-1-107	185	-0.3	32.8	2.6
Gan-1-33	158	0.62	29.5	-1.3
Gan-2-10	72	-1.36	43	0
Gan-2-13	149	0.95	57.5	-1.3
Gan-2-2	158	0.62	29.5	5.2
Gan-2-3	151	0.31	32.7	-1.3
Gan-2-5	202	0.44	64.6	-1.3
Gan-2-6	145	0.81	41.4	-3.9
Gan-2-7	122	0.45	67.8	0
Gan-2-8	107	-0.47	41.4	0
Gan-2-9	157	0.95	41.8	-1.3

B

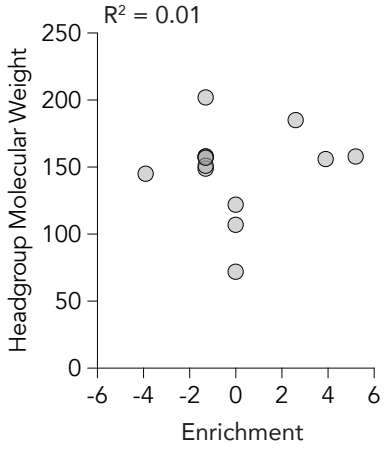

C

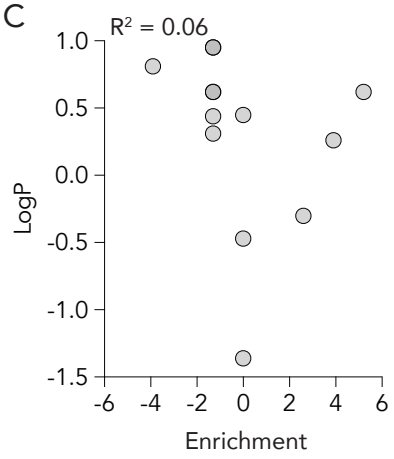

D

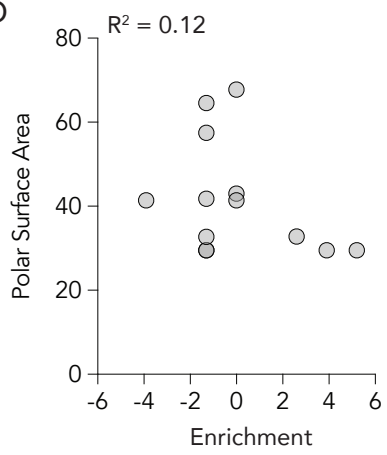

E

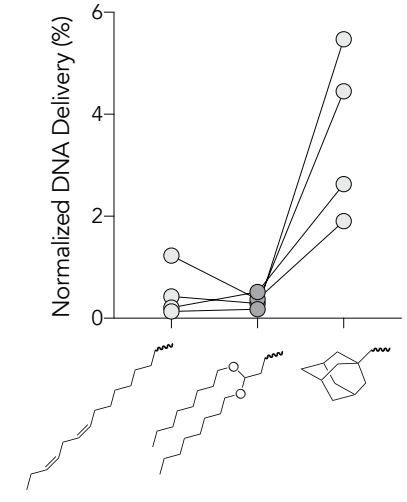

F

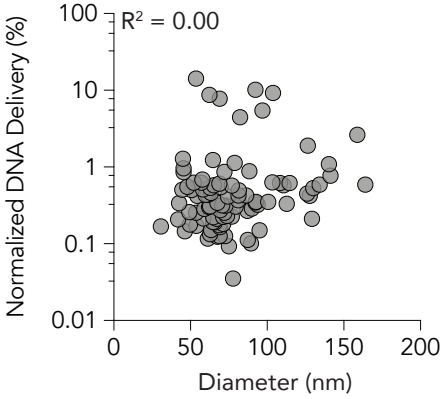

Supplementary Figure 7. Hydrodynamic diameter of LNPs plotted as a function of A) ionizable lipid type, and B) molar percent of ionizable lipid. C) Normalized delivery of in T Cells plotted against delivery show no correlations between size and delivery.

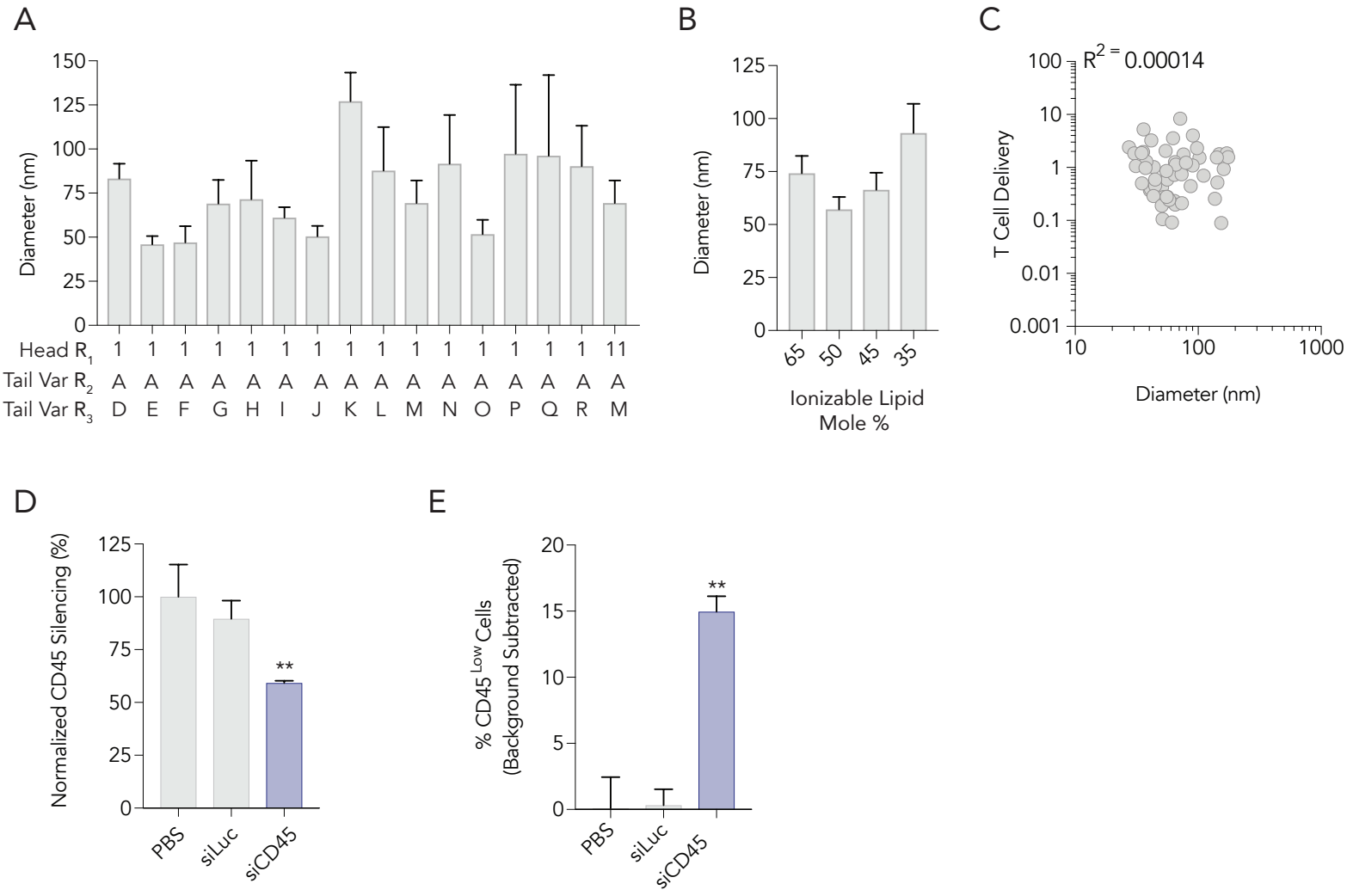
A
Diameter (nm)
150
125
100
75
50
25
0
Head R1 1 1 1 1 1 1 1 1 1 1 1 1 1 1 1 11
Tail Var R2 A A A A A A A A A A A A A A A A
Tail Var R3 D E F G H I J K L M N O P Q R M
B
Diameter (nm)
125
100
75
50
25
0
65 50 45 35
Ionizable Lipid Mole %
C
R2 = 0.00014
T Cell Delivery
100
10
1
0.1
0.01
0.001
10 100 1000
Diameter (nm)
D
Normalized CD45 Silencing (%)
125
100
75
50
25
0
**
PBS siLuc siCD45
E
% CD45 Low Cells (Background Subtracted)
20
15
10
5
0
**
PBS siLuc siCD45

Supplementary Figure 8. Normalized GFP MFI of mice treated with either PBS, cLNP carrying 1.5 mg / kg siLuc, or cLNP carrying siGFP at a dose of 0.5 or 1.5 mg / kg in A) hepatocytes, B) liver immune cells, C) liver kupffer cells, D) liver endothelial cells, E) splenic monocytes, F) splenic B cells and G) bone marrow T cells, and H) liver T cells. I) Percent of T cells found in the bone marrow and liver.

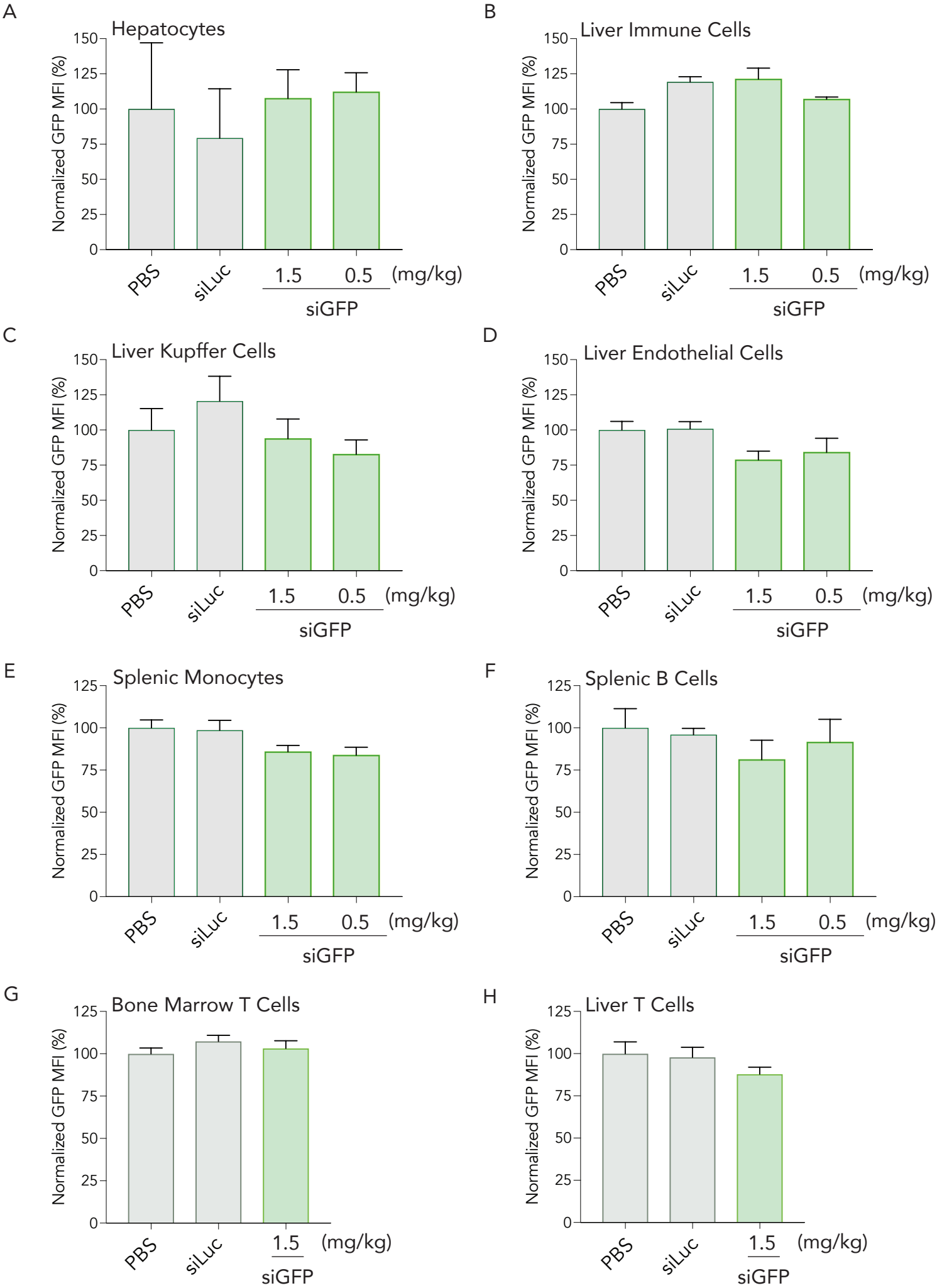
A
Hepatocytes
Normalized GFP MFI (%)
150
125
100
75
50
25
0
PBS
siLuc
1.5
0.5
(mg/kg)
siGFP
B
Liver Immune Cells
Normalized GFP MFI (%)
150
125
100
75
50
25
0
PBS
siLuc
1.5
0.5
(mg/kg)
siGFP
C
Liver Kupffer Cells
Normalized GFP MFI (%)
150
125
100
75
50
25
0
PBS
siLuc
1.5
0.5
(mg/kg)
siGFP
D
Liver Endothelial Cells
Normalized GFP MFI (%)
150
125
100
75
50
25
0
PBS
siLuc
1.5
0.5
(mg/kg)
siGFP
E
Splenic Monocytes
Normalized GFP MFI (%)
125
100
75
50
25
0
PBS
siLuc
1.5
0.5
(mg/kg)
siGFP
F
Splenic B Cells
Normalized GFP MFI (%)
125
100
75
50
25
0
PBS
siLuc
1.5
0.5
(mg/kg)
siGFP
G
Bone Marrow T Cells
Normalized GFP MFI (%)
125
100
75
50
25
0
PBS
siLuc
1.5
(mg/kg)
siGFP
H
Liver T Cells
Normalized GFP MFI (%)
125
100
75
50
25
0
PBS
siLuc
1.5
(mg/kg)
siGFP

Marrow T Cells	7.1%
Liver T Cells	6.9%

Supplementary Figure 9. A) Biodistribution of 11-A-M across 4 different cells types in the spleen and B) liver using ddPCR barcodes. C) Biodistribution of 1-A-N across 4 different cells types in the spleen and D) liver using ddPCR barcodes.

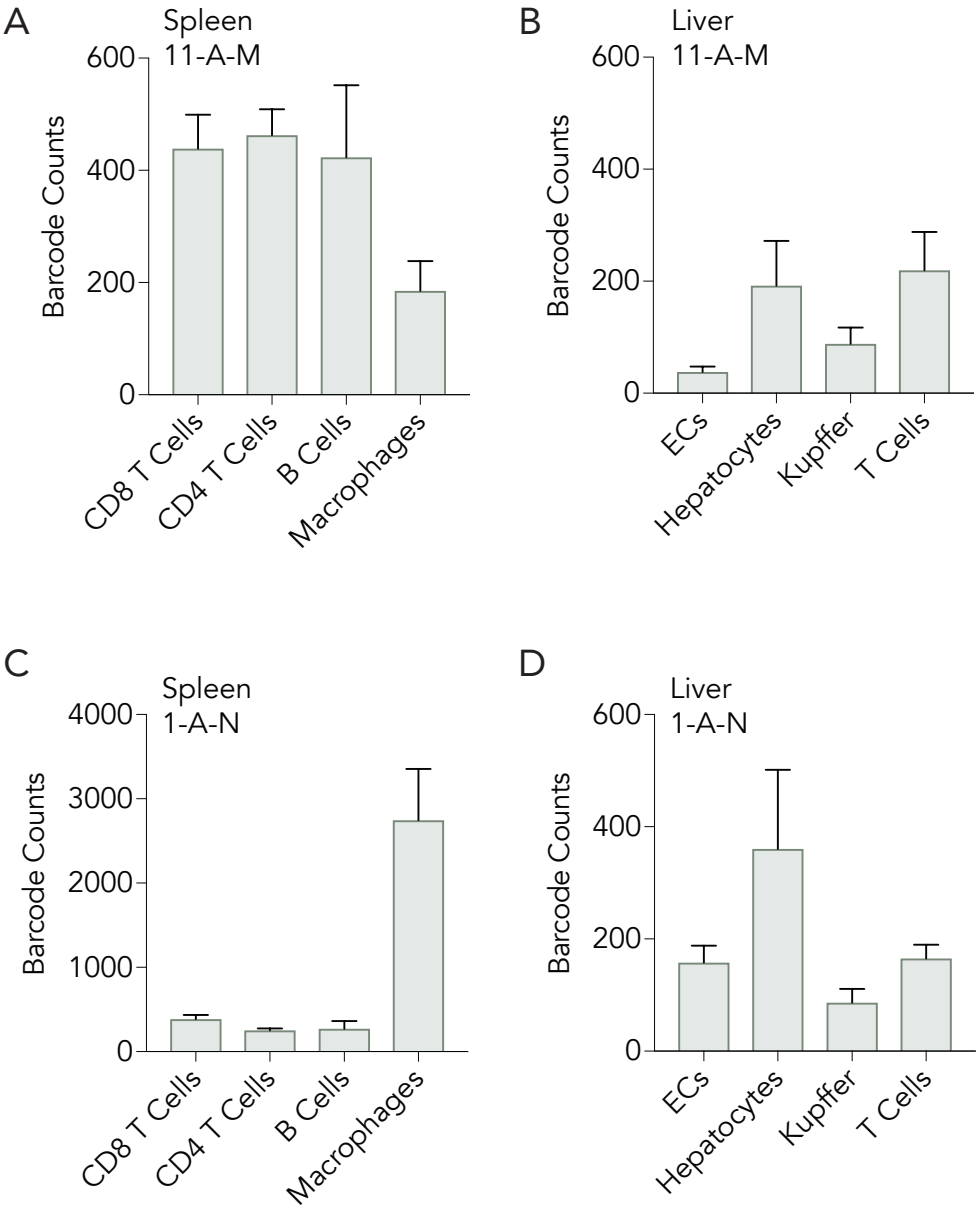
A
Spleen
11-A-M
Barcode Counts
600
400
200
0
CD8 T Cells
CD4 T Cells
B Cells
Macrophages
B
Liver
11-A-M
Barcode Counts
600
400
200
0
ECs
Hepatocytes
Kupffer
T Cells
C
Spleen
1-A-N
Barcode Counts
4000
3000
2000
1000
0
CD8 T Cells
CD4 T Cells
B Cells
Macrophages
D
Liver
1-A-N
Barcode Counts
600
400
200
0
ECs
Hepatocytes
Kupffer
T Cells

Supplementary Figure 10. A) Sequence and chemical modification for sgGFP.

sg-EGFP: 5′ - gsgsgsCGAsGsGfsAfsGfsCfUGfUfUCAfCfCGgUUUUA
GagcuagaaauagcaaGUUaAaAuAaggcuaGUccGUUAu
cAAcsususgsasasasasasgugGscascscsgsasgsuscgsg susgscsususususu - 3′

A, G, U, C: RNA nucleotide
Nf: 2′-Fluoro nucleotide
a, g, u, c: 2′-O-Methyl nucleotide s: phosphorothioate

Supplementary Figure 11. A) Encapsulation efficiency of LNP 11-A-M with siGFP.

A

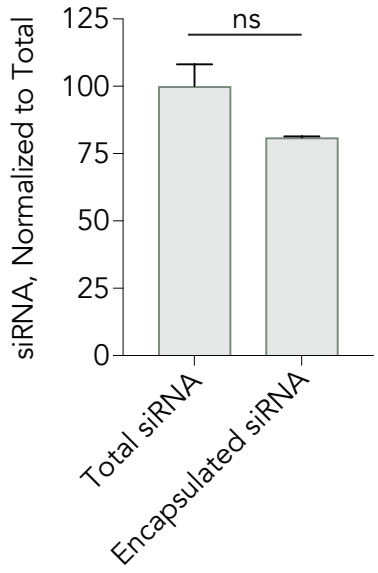
ns
125
100
75
50
25
0
siRNA, Normalized to Total
Total siRNA
Encapsulated siRNA